A Novel Tantalum Cluster Chalcohalide Ta$_4$S$_{1.5}$Se$_{7.5}$I$_8$

**Artem L. Gushchin · Maxim N. Sokolov ·
Pavel A. Abramov · Nina F. Zakharchuk ·
Vladimir P. Fedin**

Abstract Single crystals of Ta$_4$S$_{1.5}$Se$_{7.5}$I$_8$ are obtained by heating Ta, S, Se and I$_2$ at 300 °C in 4.0:1.0:8.0:4.4 molar ratio. The structure was determined by X-ray analysis and consists of molecular clusters [Ta$_4$(μ_4-S)(μ_2-Q$_{ax}$Se$_{eq}$)$_4$I$_8$] (Q $\approx$ Se$_{0.87}$S$_{0.13}$). The tantalum atoms form a square with long Ta…Ta distances (3.26–3.32 Å), with four dichalcogenide ligands bridging the Ta–Ta edges and a sulfur atom capping the square. Each Ta atom has two terminal iodine atoms. Raman spectroscopy study shows the presence of the characteristic absorption band at 396 cm^{-1} which is due to the Ta$_4$–μ_4-S vibrations. Cyclic voltammetry shows that Ta$_4$S$_{1.5}$Se$_{7.5}$I$_8$ in solid state undergoes quasi-reversible one-electron oxidation which is metal-centered.

Keywords Tantalum · Chalcogen · Chalcohalide · Cluster · Crystal structure

Introduction

For transition metals of the groups 3–8, tri- and tetranuclear cluster chalcogenide complexes can be obtained, which can be described as having a triangle (Ti, V, Mo, W, Re, Os) or square (Ln, Ta) of metal atoms, capped by a single chalcogen (Q) atom (μ_3 in the triangular and μ_4 in the square planar clusters), and bridged over each side by three (triangular clusters) or four (square planar clusters) tilted μ_2-dichalogenide

---

Please note that this article was previously published in Journal of Cluster Science, Volume 19, Number 4. This previous publication was in error. This article was originally slated to appear in this issue.

A. L. Gushchin (✉) · M. N. Sokolov · P. A. Abramov · N. F. Zakharchuk · V. P. Fedin
Nikolaev Institute of Inorganic Chemistry, Russian Academy of Sciences, 3 Lavrentiev Avenue,
Novosibirsk 630090, Russia
e-mail: gushchin_al@yahoo.com

ligands, so that $M_3Q_7^{n+}$ or $M_4Q_9^{n+}$ cluster cores result. These clusters have therefore three different chalcogen sites (one capping, one bridging, residing almost in the M_3 (or M_4) plane (so-called equatorial position) and another bridging above the same plane, on the opposite side from the capping chalcogen (termed axial chalcogens). Thus each μ_2-Q_2 ligand is represented as μ_2-$Q_{eq}Q_{ax}$. In most cases these clusters are obtained by self-assembly reactions [1–4]. This method of preparation poses an interesting problem: will this self-assembly be site-differentiating when two different chalcogen enter the core, preferentially taking a specific position each, or clusters with randomly distributed chalcogen atoms in the core would form? In fact for the trinuclear clusters it seems that the smaller chalcogen always occupies the capping position. This has been proven for the Re_2O_7/OsO_4–S–$SeCl_2$ systems which always give the $\{M_3(\mu_3$-S$)(\mu_2$-$Se_2)_3\}$ clusters [5], and for the Mo(W)–S–Se–Br_2 systems which selectively produce $\{M_3(\mu_3$-S$)(\mu_2$-$Se_2)_3\}$ clusters [A. L. Gushchin and M. N. Sokolov, unpublished results]. It turns out now that the preference of S for the capping position holds also for square clusters. Here we describe a new tetranuclear Ta cluster, $Ta_4S_{1.5}Se_{7.5}I_8$, which contains the planar Ta_4 core bridged by one μ_4-S atom, and by four μ_2-SeQ (Q $\approx$ $Se_{0.87}S_{0.13}$) units.

Experimental Section

General Procedures

High purity Ta and S powders, Se granules and I_2 crystals were used. Raman spectra were obtained by means of a Triplimate SPEX spectrometer with a 632.8 nm line of He–Ne laser for excitation. X-ray powder diffraction data were obtained on a DRON-2 powder diffractometer (CuKα radiation).

Preparation of $Ta_4S_{1.5}Se_{7.5}I_8$ (1)

Ta powder (0.36 g, 2.0 mmol), S (0.016 g, 0.5 mmol), Se (0.32 g, 4.0 mmol) and small excess of I_2 (0.55 g, 2.2 mmol) were loaded in a glass ampoule, which was evacuated, flame sealed and heated at 300 °C (4 days) in a furnace with a small natural temperature gradient. A crop of large single crystals together with a fine powder were obtained. The powder was sifted out leaving the crystals of 1. The yield was 50%. Element ratio: $Ta_{4.0}S_{1.4}Se_{7.7}I_{7.9}$ (EDAX). Raman (cm^{-1}): 396w (Ta_4–μ_4-S), 303w, 294w, 207m, 204sh, 187m, 159w, 142s, 140sh, 109s, 94s, 86vs, 73s, 70s, 65s, 59m.

Electrochemistry

As the title complex is not soluble in common solvents the electrochemical behavior was studied by the method of immobilized solid particles [6]. The cyclic volatmmograms were recorded on a 797 VA Computrance setting (Metrohm, Switzerland). A 10 mL-volume three-electrode cell was employed. As main electrode a paraffin-impregnated graphite (PIGE) with solid particles of the

complexes under investigation immobilized on it. Immobilization was achieved by rubbing crushed crystals of the complexes into the end surface of PIGE. More details concerning electrode preparation ate to be found in [7, 8]. An Ag/AgCl reference electrode, filled with 3 M KCl, was used, and auxiliary electrode was a Pt wire (6.0343 Metrohm). Background electrolyte was 0.1 M KCl, made by dissolving potassium chloride (Ultrapure) in redistilled water.

X-ray Crystallography

The diffraction data were collected on a Bruker *X8APEX* CCD diffractometer with MoKα radiation ($\lambda = 0.71073$ Å) using φ-scans of narrow (0.5°) frames. The structure was solved by direct methods and refined by full-matrix least-squares method against $|F|^2$ in anisotropic approximation with *SHELXTL* programs set. Absorption correction was applied empirically with *SADABS* program (T_{min}/$T_{max} = 0.510$) [9–11]. The detailed data are collected in Table 1.

Results and Discussion

The title compound is obtained by heating the elements in the required stoichiometric ratio at 300 °C for 4 days. It is easily separated as large black single crystals. The exact composition was determined from the X-ray data. $Ta_4S_{1.5}Se_{7.5}I_8$ is the first compound obtained in the system Ta–S–Se–I_2. The structural analogues of **1**, the selenoiodide $Ta_4Se_9I_8$ (**2**) and the thiobromide $Ta_4S_9Br_8$ (**3**) were recently obtained from the elements [1, 2].

The molecule of $Ta_4S_{1.5}Se_{7.5}I_8$ is shown in Fig. 1. The molecular structure is identical to those of **2** and **3**. Four Q_2 (Q=Se, SeS) ligands are asymmetrically coordinated to the Ta–Ta edges in the μ_2-η^2:η^2 manner. The equatorial chalcogen atoms lie almost in the Ta_4 plane, and the axial ones deviate from the plane in the opposite direction. The terminal iodine atoms are coordinated slightly asymmetrically. The interatomic distances and some angles are summarized in Table 2. The coordination polyhedron around Ta can be described as pentagonal bipyramid with μ_4-S (100 % sulfur occupancy) and one of the I atoms *trans* to it in the axial position (I_{trans}), and the two groups Q_2 and another I atom (I_{cis}) in the equatorial position. Rather long Ta–Ta distances (3.26–3.32 Å) are in agreement with the average Ta oxidation state of +4.5 in this highly electron-deficient cluster. In $Ta_4Se_9I_8$ and $Ta_4S_9Br_8$ the distances between the Ta atoms are 3.32–3.39 and 3.30 Å, respectively [1, 2]. The fact that the Ta–Ta distances in **1** and **3** are almost identical shows that the nature of the μ_4-Q atom is more decisive for the M–M distance than that of the Q_2 bridge. The Ta_4–μ_4-S bond length (2.43–2.46 Å) is practically the same as found in $Ta_4S_9Br_8$ (2.46 Å) (Table 2). The Se–Se distances correspond to single bond expected for the Se_2^{2-} formalism.

The intermolecular interactions in the crystals of $Ta_4S_{1.5}Se_{7.5}I_8$ and $Ta_4Se_9I_8$ are identical. In both **1** and **2** four shortened non-valent contacts Se_{ax}…I (3.48–3.59 Å) are all directed to the same iodine atom so that the molecules are joined into zigzag chains (Fig. 2).

Table 1 Crystallographic data and details of diffraction experiment for $Ta_4S_{1.5}Se_{7.5}I_8$

Crystal data	
Chemical formula	$Ta_4S_{1.54}Se_{7.46}I_8$
M_r	2377.41
Cell setting, space group	Orthorhombic, $Pna2_1$
Temperature (K)	150.0 (2)
a (Å)	14.3541(3)
b (Å)	14.5907(3)
c (Å)	12.9058(3)
V (Å^3)	2702.94(10)
Z	4
D_x (Mg m^{-3})	5.842
Radiation type	Mo K
μ (mm^{-1})	35.431
Crystal form, color	Plate, black
Crystal size (mm)	$0.090 \times 0.045 \times 0.025$
Data collection	
Diffractometer	Bruker X8Apex CCD detector
Data collection method	Combined ω– and phi–scans
Absorption correction	Empirical (using intensity measurements)
T_{min}	0.165
T_{max}	0.412
No. of measured, independent and observed reflections	24508, 7162, 6629
Criterion for observed reflections	$I > 2\sigma(I)$
R_{int}	0.0425
θ_{max} (°)	30.51
Refinement	
Refinement on	F^2
$R[F^2 > 2\sigma(F^2)]$, $wR(F^2)$, S	0.031, 0.061, 1.052
No. of relections	7162 reflections
No. of parameters	174
Weighting scheme	Calculated $w = 1/[\sigma^2(F_o^2) + (0.0123P)^2 + 21.0482P]$ where $P = (F_o^2 + 2F_c^2)/3$
$(\Delta/\sigma)_{max}$	0.001
$\Delta\rho_{max}$, $\Delta\rho_{min}$ (e Å^{-3})	2.325, −2.182
Extinction method	SHELXL
Absolute structure parameter	0.003(7)

The Raman spectrum of $Ta_4S_{1.5}Se_{7.5}I_8$ shows a weak band at 396 cm^{-1} that comes from Ta–μ_4-S vibrations. The position of this band correlates well with the positions of this vibration in $Ta_4S_9Br_8$ (407 cm^{-1}) [1].

Fig. 1 Molecular structure of
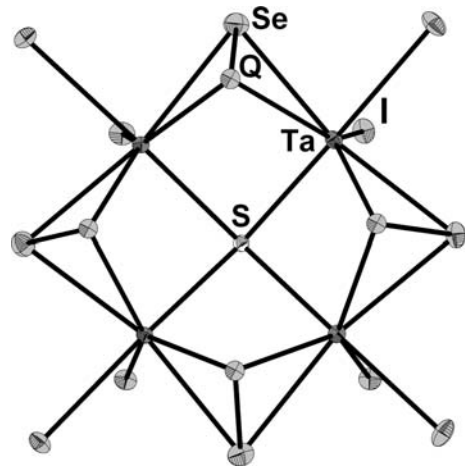$Ta_4S_{1.5}Se_{7.5}I_8$ (**1**) (ellipsoids of
50% probability level)

Table 2 Selected bond lengths [Å] for $Ta_4S_{1.5}Se_{7.5}I_8$ (**1**), $Ta_4Se_9I_8$ (**2**) and $Ta_4S_9Br_8$ (**3**)

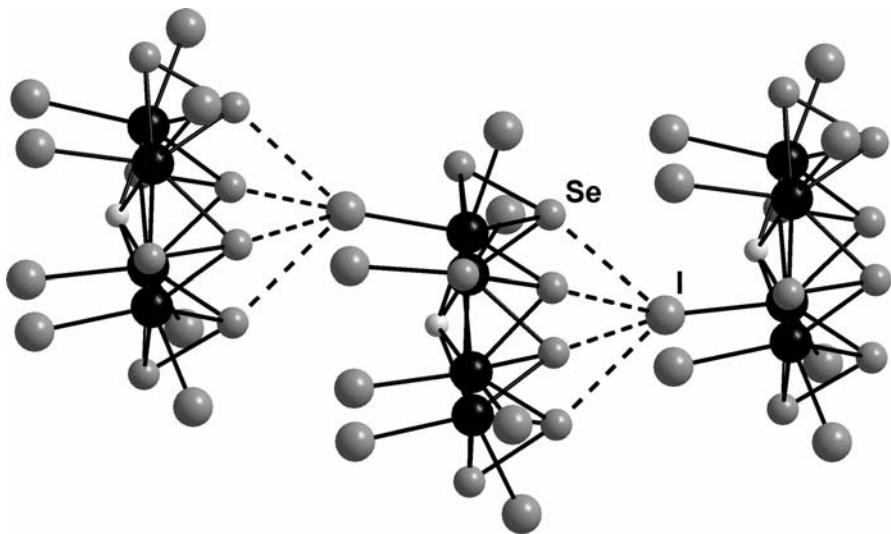| Cluster	Ta–Ta	Ta–μ_4-Q	Ta–Q	Ta–Hal	Q–Q
$Ta_4S_{1.5}Se_{7.5}I_8$	3.257(1)– 3.318(1)	2.428(3)– 2.459(3)	2.603(1)– 2.644(1)	2.715(1)– 2.785(1)	2.314(2)– 2.351(2)
$Ta_4Se_9I_8$	3.3231(4)– 3.3924(5)	2.5705(8)– 2.5978(8)	2.6003(8)– 2.6647(9)	2.7282(6)– 2.8076(5)	2.3367(11)– 2.3581(10)
$Ta_4S_9Br_8$	3.3018(15)	2.461(3)	2.500(4)– 2.521(3)	2.471(2)– 2.483(3)	2.061(8)

Fig. 2 The chains of molecules in the crystal packing of $Ta_4S_{1.5}Se_{7.5}I_8$. The short interatomic Se...I contacts are shown as dashed lines

Electrochemistry

The cyclic voltammograms of $Ta_4S_{1.5}Se_{7.5}I_8$ (**1**) mechanically immobilized on the surface of PIGE at scan rate of 20 mV s^{-1} are shown in Fig. 3. In 0.1 M KCl it exhibits a response of redox couple at $E_{1/2} = (E_m^a + E_m^c) = 0.522$ V, which is due to the transitions in the metallic core $[Ta_4]^{18+/(18+n)}$. In order to calculate the number of electrons (n) involved in the rate-determining step, a Tafel plot (Fig. 4) was drawn from background-corrected data taken from the rising part of anodic current-potential curves (where there is no concentration polarization). As is seen from Fig. 4 the Tafel plot indicates one-electron process in the rate-limiting step, assuming transfer coefficients of $\beta = 0.5$ with error not exceeding 2% (the theory requires 0.120 V/decade slope for one-electron transfer). The Tafel plot was also constructed according to the equation valid for a totally irreversible diffusion process [12], which gives $E_{1/2} = (b/2) \log v + $ Const., where b is the Tafel slope. On the basis of this equation, the slope of E_m vs lg v is $b/2 = \partial E_m/\partial \lg v$. Figure 5 shows cyclic voltammograms of $Ta_4S_{1.54}Se_{7.46}I_8$ with different scan rates and plot a maximum potential vs logarithm of scan rate for the anodic current (see inset). The $\partial E_m/\partial \lg$ v is 0.0579 V/decade, which gives $b = 2 \times 0.0579 = 0.116$ V/decade. This b value also points to one-electron transfer to be a rate-limiting step, if we assume transfer coefficient $\beta = 0.5$, with error not exceeding 2%.

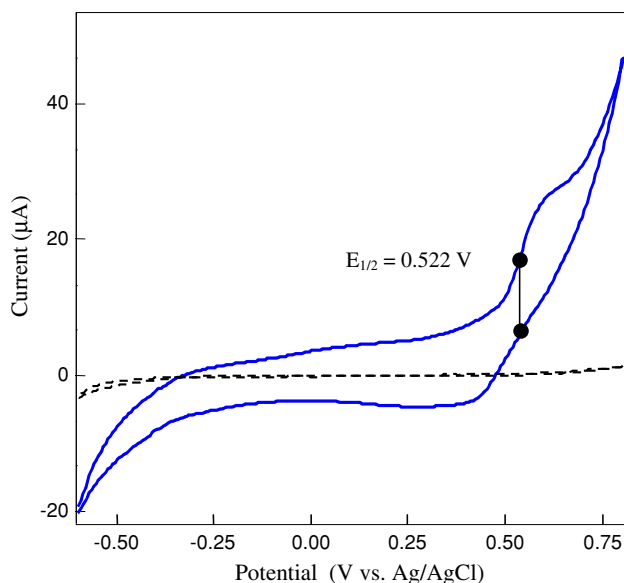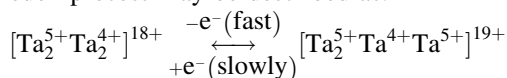Therefore, the redox-process may be described as:

$$[Ta_2^{5+}Ta_2^{4+}]^{18+} \underset{+e^-(\text{slowly})}{\overset{-e^-(\text{fast})}{\longleftrightarrow}} [Ta_2^{5+}Ta^{4+}Ta^{5+}]^{19+}$$

Fig. 3 Cyclic voltammograms of $Ta_4S_{1.5}Se_{7.5}I_8$ (**1**) mechanically immobilized on the surface of PIGE: background electrolyte 0.1 M KCl (dashed line); potential route $-0.7 \rightarrow 0.8 \rightarrow -0.7$ V; scan rate 20 mV s^{-1}

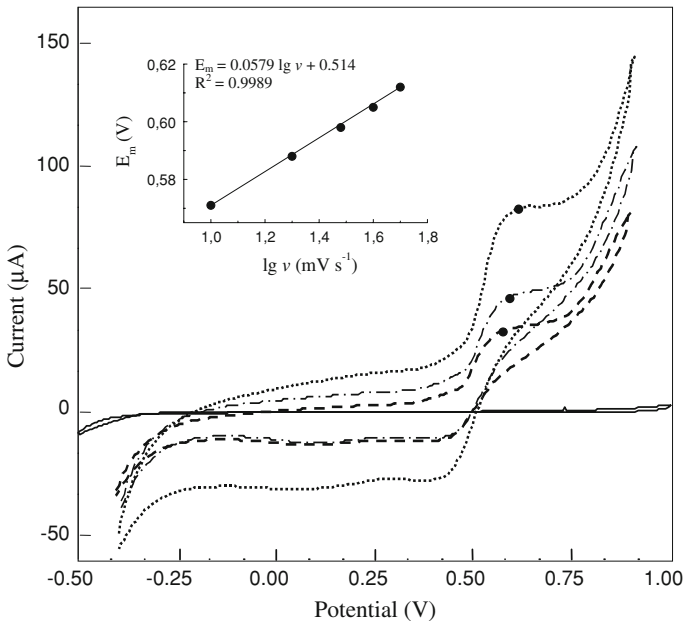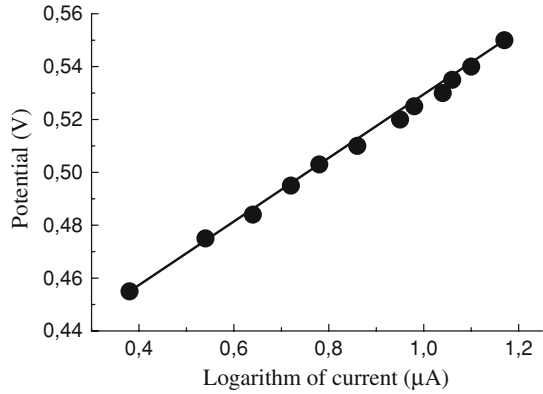**Fig. 4** Tafel plot obtained from anodic current-potential curves recoded for $Ta_4S_{1.5}Se_{7.5}I_8$ (**1**) as in Fig. 1

Fig. 5 Cyclic voltammograms of $Ta_4S_{1.5}Se_{7.5}I_8$ mechanically immobilized on the surface of PIGE (solid line): background electrolyte 0.1 M KCl; potential route $-0.3 \to 0.9 \to -0.3$ V; scan rate 10 (—), 20 (— —) and 50 ($\cdots$) mV s^{-1}. (Points denote maximum of oxidation current). *Inset* plot of maximum potential (E_m) versus logarithm of scan rate (v) for the oxidation current at the cyclic voltammograms

The results of the present study demonstrate that under self assembly conditions in a thermodynamically controlled high-temperature synthesis, the lighter chalcogen enters into a position of maximum connectivity. This agrees well with the observations made for the triangular clusters with the $\{M_3(\mu_3\text{-}Q)(\mu\text{-}Q_2)_3\}$ core [4, 5; A. L. Gushchin and M. N. Sokolov, unpublished results]. Moreover, in the structure of $Cs_4[Re_6S_{9.45}Se_{3.55}]$ the μ_3 positions in the cluster $\{Re_6(\mu_3\text{-}Q)_8\}$ are exclusively

occupied by the sulfur atoms while Se participates in the μ-Q_2 bridges between the octahedral clusters [13]. In high–temperature syntheses of cuboidal Re clusters, $\{Re_4(\mu_3\text{-}Q)_4\}$ from the elements, when two different chalcogens are introduced in the system, the lighter chalcogen invariably occupies the inner ligand site in the cluster, as for example in $Re_4S_4Te_4$ and in $Re_4S_4Cl_8(TeCl_2)_4$ [14, 15]. Thus the preference of S over Se and Te for the bridging position of maximum connectivity seems to be a general rule. A possible explanation for this systematic preference may be that the smallest size of the S maximizes the M–M bonding which is important for the overall cluster stability.

Supporting Information Available

Crystallographic data in CIF format have been deposited at Fachinformationszentrum Karlsruhe under ICSD number 419404 and can be retrieved be request (crystaldata@FIZ-Karlsruhe.de).

References

1. M. N. Sokolov, A. L. Gushchin, P. A. Abramov, A. V. Virovets, E. V. Peresypkina, S. G. Kozlova, B. A. Kolesov, C. Vicent, and V. P. Fedin (2005). *Inorg. Chem.* **44**, 8756.
2. M. N. Sokolov, A. L. Gushchin, A. V. Virovets, E. V. Peresypkina, S. G. Kozlova, and V. P. Fedin (2004). *Inorg. Chem.* **43**, 7966.
3. M. N. Sokolov, V. P. Fedin, and A. G. Sykes (2003). *Compr. Coord. Chem. II* **4**, 768.
4. V. E. Fedorov, Y. V. Mironov, N. G. Naumov, M. N. Sokolov, and V. P. Fedin (2007). *Russ. Chem. Bull.* **76**, 529.
5. S. V. Volkov, Z. A. Fokina, O. G. Yanko, V. I. Pekhnyo, and L. B. Kharkova (2005). *Zh. Neorg. Khim.* **50**, 1244.
6. F. Scholz and B. Meyer in A. J. Bard, and I. Rubenstein (eds.), *Voltammetry of Solid Microparticles Immobilized on Electrode Surfaces, Electroanalytical Chemistry. A Series of Advances*, vol. 20 (Dekker, New York Basel Hong-Kong, 1998), pp. 1–86.
7. F. Scholz and B. Meyer (1994). *Chem. Soc. Rev.* **23**, 341.
8. N. Zakharchuk, B. Meyer, H. Hennig, F. Scholz, A. Jaworksi, and Z. Stojek (1995). *J. Electroanal. Chem.* **398**, 23.
9. Bruker AXS Inc *SADABS (Version 2.11)* (Bruker Advanced X-ray Solutions, Madison, Wisconsin, USA, 2004).
10. G. M. Sheldrick *SHELX-97* (Universität Göttingen, Germany, 1997).
11. L. J. Farrugia ORTEP-3 (Department of Chemistry, University of Glasgow, 1997).
12. A. J. Bard and I. R. Faulkner, *Electrochemical Methods, Fundamentals and Applications* (Wiley, New York, 2001).
13. W. Bronger, H.-J. Miessen, R. Neugröshel, D. Schmitz, and M. Spangenberg (1985). *Z. Anorg. Allg. Chem.* **525**, 41.
14. Y. V. Mironov, T. E. Albrecht-Schmitt, and J. A. Ibers (1997). *Inorg. Chem.* **36**, 944.
15. V. E. Fedorov, Y. V. Mironov, V. P. Fedin, H. Imoto, and T. Saito (1996). *Acta Crystallogr. Sect. C* **52**, 1065.